

# Dual-beam incoherent cross-correlation spectroscopy

K.-Q. Xia and Y.-B. Xin

*Department of Physics, The Chinese University of Hong Kong, Shatin, New Territories, Hong Kong*

P. Tong

*Department of Physics, Oklahoma State University, Stillwater, Oklahoma 74078*

Received January 3, 1995; accepted February 8, 1995

An incoherent dynamic light-scattering technique is developed to measure the local velocity and its statistics. By employing two parallel laser beams of different colors, the technique measures the cross-correlation function of the scattered intensities from two separate illuminating volumes. Because there is no phase coherence between the two laser beams, the measured cross-correlation function is sensitive only to the intensity fluctuations caused by a seed particle that crosses the two beams in succession. The flow velocity is obtained from the measured particle transit time. We frame the scattering theory so as to account for the two-beam scattering geometry. Our experiment verifies the calculation and demonstrates applications of the technique. The method has the unique feature of being able to measure simultaneously the local velocity in two opposite directions perpendicular to the incident laser beams. Its advantages are high spatial resolution and accuracy, fast temporal response, and ease of use. The technique is useful in studies of turbulent flows, sedimentation of heavy particles, and flow phenomena in complex fluids.

## 1. INTRODUCTION

In recent years there has been a growing interest in studying turbulence in simple fluids and nonlinear flow phenomena in complex fluids. Examples of these studies include turbulent Rayleigh–Bénard convection,<sup>1</sup> sedimentation of colloidal particles,<sup>2</sup> and small convective flows in binary liquid mixtures near the critical points.<sup>3</sup> Many experimental methods have been used to measure velocity fluctuations in these systems; a standard one is laser Doppler velocimetry (LDV).<sup>4</sup> With the LDV scheme, one focuses two coherent laser beams to a small spatial point at which the two beams form interference fringes. When a seed particle traverses the crossover region, the scattering of the seed particle is modulated by the interference fringes with a frequency proportional to the velocity of the particle. Under certain unfavorable conditions, however, the application of LDV is limited. For example, in combustion and strong thermal convection, fluctuations of the fluid refractive index resulting from large temperature fluctuations may cause the laser beam to wander and defocus in the turbulent fluid and therefore to perturb the crossing of the two laser beams used in LDV. Because it can permit only one particle in the scattering volume at a given time, LDV is also limited in measuring the flow velocity near a solid wall or in polymer solutions and other complex fluids, where strong background scattering may ruin the LDV signal.

In this paper we present a new light-scattering technique, which can be used to measure accurately the local velocity and its statistics in these complex systems. The principle of the technique is simple—it involves measuring the time for a small seed particle having a velocity  $v$  in the flow field to cross two parallel laser beams. The two laser beams have different colors and are separated by a known distance  $l$  ( $\sim 0.1$  mm). Experimentally this transit time, or delay time, is determined from the intensity

cross-correlation function

$$g_c(t) = \frac{\langle I_b(t')I_g(t'+t) \rangle}{\langle I_b \rangle \langle I_g \rangle},$$

where  $I_b$  and  $I_g$  are the scattered light intensities from the two parallel beams termed blue and green, respectively. In the experiment to be described below, the two beams are the blue light and the green light from an argon-ion laser. Because there is no phase coherence between  $I_b$  and  $I_g$ , the function  $g_c(t)$  is sensitive only to the scattering-amplitude fluctuations produced by the seed particles moving in and out of the scattering volumes. This method takes advantage of the laser source while avoiding its coherence by using the two-color cross-correlation scheme.

The method is an extension of our recently developed technique of incoherent cross-correlation spectroscopy,<sup>5</sup> in which a single laser beam consisting of two colors is used. Because of the radial symmetry of the laser-beam profile, the single-beam method can measure only the square of the velocity components perpendicular to the beam. Since it can distinguish which of the two parallel beams the seed particle traverses first, the dual-beam method is sensitive to the flow direction. By simultaneously measuring the two cross-correlation functions  $\langle I_b(t')I_g(t'+t) \rangle$  (blue cross green) and  $\langle I_g(t')I_b(t'+t) \rangle$  (green cross blue), one can distinguish flows in two opposite directions perpendicularly across the two incident laser beams. This feature is unique in studies of turbulent flows in which the technique can be used to measure the velocity probability density functions  $P(v)$  and  $P(-v)$  simultaneously.

The idea of measuring time of flight between two small volumes in space for flow measurements has been explored by several authors; some directly detect the separation between two consecutive pulses as a measure of the time of flight<sup>6–8</sup>; others use various kinds of correlation

schemes.<sup>9-11</sup> Because of the limitations of the receiving electronic, the early time-of-flight methods could detect only large intensity fluctuations produced by a single (large) seed particle. The local velocity was determined on the basis of individual scattering events, and no probability distribution of the velocity was obtained. With a new digital correlator and the cross-correlation scheme, we are able to measure small intensity fluctuations produced by many particles moving in and out of the scattering volumes. We frame the scattering theory so as to encompass fluctuations in the number of particles in the scattering volumes. By signal averaging a large number of intensity fluctuations, one can obtain the exact functional form of  $g_c(t)$  with high statistical accuracy. The probability density function  $P(v)$  for the local velocity  $v$  can then be deduced from the measured  $g_c(t)$ .

Our two-color cross-correlation scheme is capable of measuring the scattering-amplitude fluctuations with a cutoff frequency up to 10 MHz and a spatial resolution better than 60  $\mu\text{m}$ . The experimental uncertainties are essentially statistical. At a moderately high scattering intensity ( $I \sim 10^4$  counts/s), it takes only  $\sim 5$  min to collect data with an adequate signal-to-noise ratio. Since an incoherent detecting method is used, an increasing number of particles in the scattering volume tends to average out the scattering-amplitude fluctuations. In fact, as will be shown below,  $g_c(t)$  goes as  $1/\bar{N}$ , where  $\bar{N}$  is the average number of particles in the scattering volume. In our experimental arrangement the particle number in the scattering volume can be controlled in the range  $1 < \bar{N} < 100$ , and therefore the smallest signal-to-noise ratio [evaluated by the value of  $g_c(t)$  at time  $t = 0$ ] is at the 1% level. Because of the small signal-to-noise ratio, it is difficult to measure  $g_c(t)$  by using normal commercial correlators. The new correlator used in the experiment is the ALV-5000 multiple- $\tau$  correlator, which utilizes a symmetric normalization technique, making it much easier to probe incoherent fluctuations with small amplitudes and long relaxation times. The ALV-5000 correlator is capable of measuring fluctuating signals with a signal-to-noise ratio as low as 0.1%. It should be pointed out that the present technique is not meant to replace LDV, particle imaging velocimetry, and other time-of-flight velocimeters; rather, it should be used to complement these techniques. Our cross-correlation method is particularly useful for measuring the local velocity and its statistics in situations in which either vibrations or refractive-index fluctuations may cause the laser beam to wander in the fluids or there is a strong background scattering from a nearby wall or in polymer solutions and other complex fluids.

Section 2 contains theoretical calculations for particle-number fluctuations involving two scattering volumes. Experimental details appear in Section 3, and the results are presented and analyzed in Section 4. A brief comparison between the present technique and LDV as well as other time-of-flight methods is also made in Section 4. Finally, the work is summarized in Section 5.

## 2. THEORY

The basic dynamic light-scattering theory for coherent and incoherent sources is well documented.<sup>12,13</sup> Here we

reframe the theory so as to account for a new scattering geometry involving two parallel laser beams of different colors (say, blue and green) with a small separation  $l$ . We calculate the intensity cross-correlation function

$$g_c(t) = \frac{\langle E_b^*(t')E_b(t')E_g^*(t'+t)E_g(t'+t) \rangle}{\langle E_b^*(t')E_b(t') \rangle \langle E_g^*(t')E_g(t') \rangle} = \frac{K}{\langle I_b(t') \rangle \langle I_g(t') \rangle}, \quad (1)$$

where the angle brackets represent a time average over  $t'$  and  $t$  is the delay time. In the experiment to be described below, the two scattering intensities  $I_b(t)$  and  $I_g(t)$  are measured from two separate scattering volumes,  $V_b$  and  $V_g$ , respectively. We will focus on fluctuations in the number of seed particles in the scattering volumes and discuss the application of the technique in velocimetry.

Let us now consider scattering by uniform spherical solid particles, which scatter light isotropically. The scattered electric field can be written as<sup>14</sup>

$$E(t) = \sum_{j=1}^{N_0} a_j(t) \exp[-i\mathbf{q} \cdot \mathbf{r}_j(t)], \quad (2)$$

where  $N_0$  is the total number of particles in the fluid,  $a_j(t)$  is the scattering amplitude of the  $j$ th particle, and  $\mathbf{r}_j(t)$  is the position of the particle at time  $t$ . For an isotropic particle with a fixed scattering cross section,  $a_j(t)$  changes with time continuously because the scattering of the particle varies as the particle changes its position in a nonuniformly illuminated scattering volume. If the scattering volume is uniformly illuminated, this amplitude will take a constant value when the particle is in the scattering volume and will become zero when the particle leaves the scattering volume. In Eq. (2) the polarization of the incident light is assumed to be perpendicular to the scattering plane, and a proportionality constant has been omitted for simplicity. The photon momentum-transfer vector  $\mathbf{q}$  has an amplitude  $q = (4\pi n/\lambda_0)\sin(\theta/2)$ , where  $\theta$  is the scattering angle,  $n$  is the refractive index of the fluid, and  $\lambda_0$  is the wavelength of the incident light.

With Eq. (2) one finds that the function  $K$  in Eq. (1) has the form<sup>5</sup>

$$K = \sum_{i,j,k,l}^{N_0} \langle a_i^b(t')a_j^b(t')a_k^g(t'+t)a_l^g(t'+t) \rangle \times \langle \exp\{-i\mathbf{q}_b \cdot [\mathbf{r}_i(t') - \mathbf{r}_j(t')] - i\mathbf{q}_g \cdot [\mathbf{r}_k(t'+t) - \mathbf{r}_l(t'+t)]\} \rangle, \quad (3)$$

where the superscripts  $b$  and  $g$  denote the blue and the green beams, respectively. In the above, we have assumed that the phase and amplitude fluctuations of the scattered light are statistically independent. This decoupling approximation is valid because the time scales involved in the two processes are usually widely separated. Because of the random distribution of the particles in the fluid, the only terms that survive the ensemble average in Eq. (3) must satisfy one of the following four conditions<sup>5</sup>: (1)  $i = j = k = l$  for arbitrary nonzero  $\mathbf{q}_b$  and  $\mathbf{q}_g$ , (2)  $i = j \neq k = l$  for arbitrary nonzero  $\mathbf{q}_b$  and  $\mathbf{q}_g$ , (3)  $i = l \neq j = k$  for  $\mathbf{q}_b = \mathbf{q}_g \neq 0$ , or (4)  $i = k \neq j = l$  for  $\mathbf{q}_b = -\mathbf{q}_g \neq 0$ . Equation (3) then becomes

$$\begin{aligned}
K &= \sum_{i=1}^{N_0} \langle A_i^b(t') A_i^g(t' + t) \rangle + \sum_{i \neq j}^{N_0} \langle A_i^b(t') A_j^g(t' + t) \rangle \\
&+ \sum_{i \neq j}^{N_0} \langle a_i^b(t') a_i^g(t' + t) a_j^b(t') a_j^g(t' + t) \rangle \\
&\times |F_s(\mathbf{q}, t)|^2, \tag{4}
\end{aligned}$$

where  $A_i(t) = a_i^2(t)$  and the function  $F_s(\mathbf{q}, t) = \langle \exp\{-i\mathbf{q} \cdot [\mathbf{r}(t') - \mathbf{r}(t' + t)]\} \rangle$ , which arises from the interference of the coherent fields scattered by the moving particles. Condition (3) or (4) gives rise to  $F_s(\mathbf{q}, t)$ . In dynamic light scattering this phase-fluctuation term is usually measured to study diffusive motions of small particles<sup>12,15</sup> and fluid dynamics in laminar<sup>16</sup> and turbulent<sup>17</sup> flows. In our incoherent cross-correlation scheme, neither the condition  $\mathbf{q}_b = \mathbf{q}_g$  nor  $\mathbf{q}_b = -\mathbf{q}_g$  is met, and therefore  $F_s(\mathbf{q}, t) = 0$ . We will subsequently drop this term.

We now focus on the first two terms in Eq. (4), which are from condition (1) ( $i = j = k = l$ ) and condition (2) ( $i = j \neq k = l$ ), respectively. Notice that these two terms are independent of the photon momentum-transfer vector  $\mathbf{q}$ , because they arise from amplitude fluctuations of the scattered light. By writing the scattering power  $A(t)$  as a sum of its average value  $\bar{A}$  and the fluctuation  $\delta A(t)$  from  $\bar{A}$  [i.e.,  $A(t) = \bar{A} + \delta A(t)$ ], we have

$$\begin{aligned}
K &= (N_0)^2 \bar{A}^b \bar{A}^g + N_0 \langle \delta A_1^b(t') A_1^g(t' + t) \rangle \\
&+ N_0(N_0 - 1) \langle \delta A_1^b(t') \delta A_2^g(t' + t) \rangle, \tag{5}
\end{aligned}$$

where subscript 1 in the second term denotes that the correlation function is from a single particle and subscripts 1 and 2 in the third term denote that it is from a pair of particles. Again, we have assumed that all particles behave the same statistically. Similarly to the case with Eq. (3), one can show<sup>5</sup> that in Eq. (1) the average scattering intensities  $\langle I_b(t') \rangle = N_0 \bar{A}^b$  and  $\langle I_g(t') \rangle = N_0 \bar{A}^g$ . Substituting these results and Eq. (5) into Eq. (1), we have

$$\begin{aligned}
g_c(t) &= 1 + \frac{\langle \delta A_1^b(t') \delta A_1^g(t' + t) \rangle}{N_0 \bar{A}^b \bar{A}^g} \\
&+ \frac{(N_0 - 1) \langle \delta A_1^b(t') \delta A_2^g(t' + t) \rangle}{N_0 \bar{A}^b \bar{A}^g} \\
&= 1 + g_{NS}(t) + g_{NT}(t). \tag{6}
\end{aligned}$$

It should be pointed out that both  $g_{NS}(t)$  and  $g_{NT}(t)$  measure the correlation between fluctuations in the number of particles in the two scattering volumes  $V_b$  and  $V_g$ . The difference between them is as follows:  $g_{NS}(t)$  is caused by a single particle, which is in  $V_b$  at time  $t'$  and visits  $V_g$  at a later time  $t' + t$ . The correlation function  $g_{NT}(t)$ , on the other hand, is caused by two different particles; one of them is in  $V_b$  at time  $t'$  and the other is in  $V_g$  at a delay time  $t' + t$ . We therefore call  $g_{NS}(t)$  the single-particle (or self) number-fluctuation correlation function and  $g_{NT}(t)$  the two-particle (or pair) number-fluctuation correlation function.

When the particles in the fluid are randomly distributed, there is no correlation between the number fluctuations in the two scattering volumes, and therefore  $g_{NT}(t) = 0$ . The correlation function  $g_{NT}(t)$  becomes nonzero only when there exists a spatial coherence among

the particles in the fluid. Such a spatial coherence can be found in a colloidal crystal in which all the colloidal particles form a lattice in the solvent.<sup>18,19</sup> An advantage of using the two-beam scheme is that one can measure  $g_{NS}(t)$  and  $g_{NT}(t)$  individually by changing the orientation of the plane defined by the two parallel laser beams. When the flow direction is not perpendicular to the normal direction of the two-beam plane, the single-particle correlation function  $g_{NS}(t) = 0$  and the measured correlation function is simply the two-particle correlation function  $g_{NT}(t)$ . If the two scattering volumes coincide (single-beam geometry, which was used in most previous studies of number fluctuations<sup>5,13</sup>), one cannot distinguish  $g_{NS}(t)$  and  $g_{NT}(t)$  even when there is a spatial coherence among the particles.

For two laser beams having intensity profiles  $I_b(\mathbf{r})$  and  $I_g(\mathbf{r})$ , the correlation function  $g_{NS}(t)$  can be written as<sup>13,20</sup>

$$g_{NS}(t) = \frac{1}{N_0} \frac{1/V \int d^3\mathbf{r} \int d^3\mathbf{r}_0 I_b(\mathbf{r}) I_g(\mathbf{r}_0) P(\mathbf{r} - \mathbf{r}_0; t)}{(1/V)^2 \int I_b(\mathbf{r}) d^3\mathbf{r} \int I_g(\mathbf{r}) d^3\mathbf{r}}, \tag{7}$$

where  $V$  is the total volume of the scattering sample and  $P(\mathbf{r} - \mathbf{r}_0; t)$  is the probability density for a particle to move from  $\mathbf{r}_0$  to  $\mathbf{r}$  in a time  $t$ . In a typical laser-scattering experiment, the scattering volume has a thin cylindrical shape, with its length  $L$ , defined by a slit in the detecting optics, being larger than its waist radius. A laser beam usually has a Gaussian intensity profile

$$I(\mathbf{r}) = I_0 \exp[-2(r_\perp/\sigma)^2], \tag{8}$$

where  $r_\perp$  is the radial distance from the center of the laser beam and  $\sigma$  is the beam radius at which the intensity falls to  $1/e^2$  of its maximum value  $I_0$  at the center of the beam.

The probability density function  $P(\mathbf{r} - \mathbf{r}_0; t)$  characterizes the dynamics of the probe particles in the fluid. When the particles move with a uniform velocity  $\mathbf{v}$ , the probability density function  $\mathbf{P}(\mathbf{r} - \mathbf{r}_0; t)$  takes the form

$$\mathbf{P}(\mathbf{r} - \mathbf{r}_0; t) = \delta(x - x_0 - vt) \delta(y - y_0) \delta(z - z_0). \tag{9}$$

In the above, we have assumed that  $\mathbf{v} = v\hat{x}$ , and a coordinate system is chosen such that the blue beam coincides with the  $z$  axis and the green beam is parallel to the  $z$  axis, at  $x = l$  and  $y = 0$ . Substituting Eqs. (8) and (9) into Eq. (7), we obtain

$$\begin{aligned}
g_{NS}(t) &= \frac{1}{N} \exp\left[\frac{-(vt - l)^2}{\sigma^2}\right] \\
&= \frac{1}{N} \exp\left[-2\left(\frac{t - t_0}{\sqrt{2}\sigma/v}\right)^2\right], \tag{10}
\end{aligned}$$

where  $\sigma^2 = (\sigma_1^2 + \sigma_2^2)/2$ , with  $\sigma_1$  and  $\sigma_2$  being the  $1/e^2$  radii of the blue and the green beams, respectively, and  $N = N_0(\bar{V}_s/V)$  is the average number of the particles in the average scattering volume  $\bar{V}_s = (V_b + V_g)/2 = \pi L(\sigma_1^2 + \sigma_2^2)/2$ . Here,  $L$  is the length of the scattering volumes as defined by the slit width (see Section 3). In

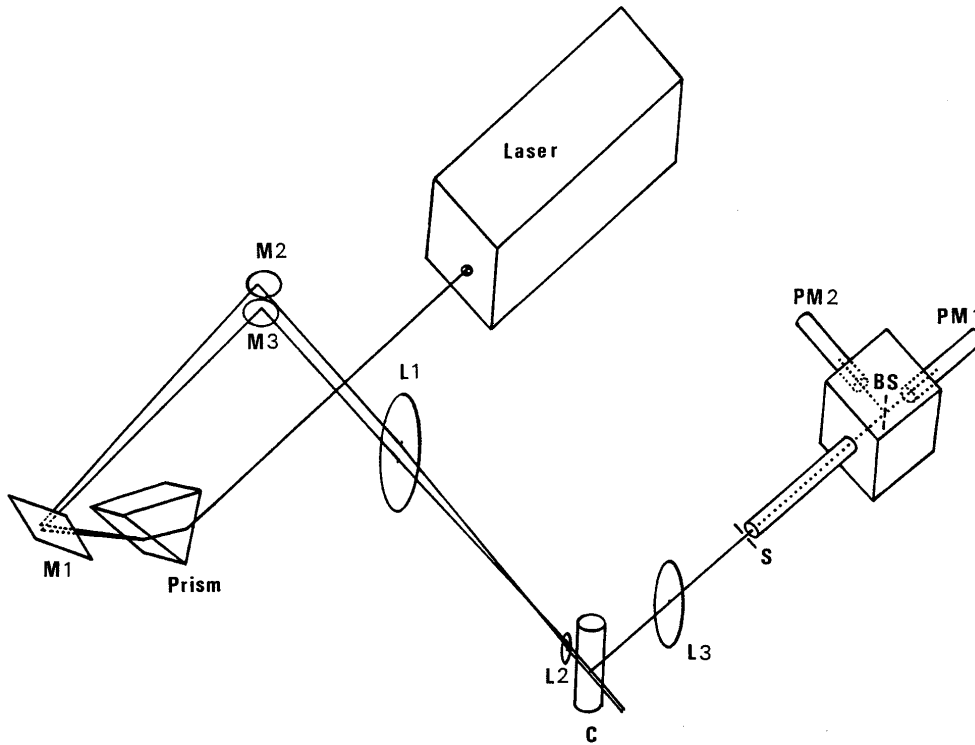


Fig. 1. Schematic diagram of the experimental setup: M1, M2, and M3, mirrors; L1, L2, and L3, lenses; S, adjustable slit; BS, beam splitter; PM1 and PM2, photomultipliers; and C, scattering cell (drawing not to scale).

Eq. (10)  $t_0 = l/v$  is the time for a particle having a velocity  $v$  to cross the two parallel laser beams with a separation  $l$ . Equation (10) clearly shows that the correlation function  $g_{NS}(t)$  is a Gaussian function centered at the delay time  $t_0$  with a  $1/e^2$  half-width  $\sqrt{2}\sigma/v$ . The height of the Gaussian peak is proportional to  $1/\bar{N}$ , where  $\bar{N}$  is the average number of particles in the scattering volume. When the separation  $l = 0$ , Eq. (10) agrees with our previous result.<sup>5</sup>

For a turbulent flow we have

$$g_{NS}(t) = \frac{1}{\bar{N}} \int dv P(v) \exp\left[-\frac{(vt - l)^2}{\sigma^2}\right], \quad (11)$$

where  $P(v)$  is the probability density function of the local velocity  $v$  in the direction perpendicular to the laser beams. In the above, the flow velocity is measured over the distance  $l$  between the two parallel laser beams. In a typical experimental arrangement,  $l$  can be reduced to  $\sim 50 \mu\text{m}$ . The measured local velocity is also averaged over the length  $L$  of the two scattering volumes viewed by the photodetectors. In our experiment the length of the scattering volume is  $\sim 50 \mu\text{m}$ . By changing the direction of the incident laser beams, one can measure the local velocity in different directions. For a fixed beam orientation our technique is capable of distinguishing  $v$  and  $-v$ , the local velocities in the direction perpendicular to the two laser beams. This is because the time delay between the intensity fluctuations in the two scattering volumes, introduced by a particle crossing the two laser beams, is unidirectional. Therefore one can obtain the probability density functions  $P(v)$  and  $P(-v)$  by measuring the intensity cross-correlation functions  $\langle I_b(t')I_g(t' + t) \rangle$  (blue cross green) and  $\langle I_g(t')I_b(t' + t) \rangle$  (green cross blue), respectively.

### 3. EXPERIMENT

Figure 1 shows the experimental setup. The argon-ion laser (Coherent Innova-70) was under multiline operation with a wavelength range from 457.9 to 514.5 nm. The laser beam was first incident upon a prism, and the dispersed beams of different colors were reflected by a mirror, M1, at a higher elevation. Two small mirrors, M2 and M3, mounted above the original laser beam were then used to intercept the blue (488.0-nm) and the green (514.5-nm) beams, while other less-intensive beams (not shown in the figure) were allowed to pass through the edges of the two mirrors or were blocked before they reached the two mirrors. The blue and the green beams intercepted by M2 and M3 were reflected at  $90^\circ$  with respect to the original laser-beam direction. The orientations of the two mirrors were individually adjusted so that the two beams became parallel to each other after reflection. One can vary the separation of the two parallel beams, which was 8 mm in our setup, by changing the mirror heights and the interception distances of the three mirrors. The diameters and the separation of the two parallel beams were then further reduced by a beam reducer (a reverse beam expander) consisting of a pair of achromatic lenses, L1 and L2. The focal lengths of L1 and L2 were 500 and 10 mm, respectively, and the distance between the two lenses was adjusted to be the sum of their focal lengths (510 mm). This arrangement gave a reduction ratio of 50. Using the measured values of the beam radii (2 mm) and the beam separation (8 mm) at the entrance of L1 together with the reduction ratio, we calculated the beam radii and separation at the exit of L2 to be 0.05 and 0.16 mm, respectively. These two beam parameters were verified from the measured intensity profile of the two laser beams. We measured the beam

profile by using a micrometer-controlled translation stage, a small pinhole ( $\sim 5 \mu\text{m}$  in diameter), and a photodiode.

The two parallel beams were incident upon a flow cell, C, placed closely behind L2. Lens L3 with a focal length  $f = 100 \text{ mm}$  was placed at a  $90^\circ$  scattering angle and at a distance  $2f$  from the flow cell, so that it projected the scattered laser beams in the flow cell onto an adjustable slit, S, with a 1:1 magnification. The slit width  $L$  together with the beam diameters determine the scattering volumes to be viewed by the photodetectors. A typical slit width used in our experiment was  $0.05 \text{ mm}$ . Light passing through the slit fell into a pinhole  $0.6 \text{ mm}$  in diameter. Two photomultiplier tubes, PM1 and PM2, were mounted at a right angle on a cubic box, which was connected to the pinhole by a  $400\text{-mm}$ -long metal tube. This arrangement ensured that only the scattered light passing through the slit could be viewed by the two PM tubes. The beam splitter, BS, at the center of the box had a reflection-to-transmission ratio of 50/50. An interference filter (not shown in the figure) was placed in front of each PM tube. The center wavelengths of the two filters were  $488.0$  and  $514.5 \text{ nm}$ . Both filters had a bandwidth, full width at half-maximum, of  $1 \text{ nm}$ .

The pulse trains from the two photomultipliers were fed to an ALV-5000 correlator whose output gives the intensity cross-correlation function,

$$g_c(t) = \frac{\langle I_b(t')I_g(t'+t) \rangle}{\langle I_b(t') \rangle \langle I_g(t') \rangle} = 1 + \beta G_c(t), \quad (12)$$

where  $I_b$  and  $I_g$  are the scattering intensities of the blue light and the green light, respectively, and  $\beta$  is a constant that depends on the geometry of the experimental setup. Because there is no phase coherence between the blue light and the green light, the function  $G_c(t)$  in Eq. (12) is simply  $g_{NS}(t) + g_{NT}(t)$ . In our experiment the seed particles were randomly distributed in the fluid, so that  $g_{NT}(t) = 0$  and therefore  $g_c(t) = 1 + \beta g_{NS}(t)$ . The ALV-5000 multiple- $\tau$  correlator used to measure  $g_c(t)$  had a fixed range of delay times between  $0.2 \mu\text{s}$  and  $1 \text{ h}$ .

Our flow cell was a section of glass tube,  $70 \text{ cm}$  in length,  $3.6 \text{ mm}$  in inner diameter, and  $6.0 \text{ mm}$  in outer diameter. The tube was placed vertically so that the flow lines were perpendicular to the incident laser beams and lay in the plane defined by the two beams. The long glass tube chosen for the experiment ensured that our flow measurements were conducted in a well-developed laminar-flow region. The fluid used in the experiment was distilled water filtered by  $0.22\text{-}\mu\text{m}$  filters. Monodispersed latex spheres  $0.55 \mu\text{m}$  in diameter were used as the seed particles. To measure the concentration dependence of  $g_{NS}(t)$  [see Eq. (10)] we varied the volume fraction of the particles between  $1 \times 10^{-7}$  and  $3 \times 10^{-5}$ . We verified that in this concentration range, the particle interaction can be ignored. All measurements were made at room temperature. With a magnetically coupled pump (Micropump Model 1316SS), the aqueous solution of the latex spheres was pumped through the tube at different flow rates.

#### 4. RESULTS AND DISCUSSION

To test the technique, we first performed the cross-correlation-function measurements in a laminar flow with

a constant flow rate  $J$ . The flow was set such that the seed particles would first pass the green beam and then the blue one. The slit S ( $0.05 \text{ mm}$  in width) shown in Fig. 1 was positioned in such a way that only the scattering from the center of the pipe could be viewed by the photodetectors. Therefore the flow velocity  $V_0$  at the center of the pipe was measured. Figure 2 shows two cross-correlation functions measured simultaneously by our correlator operated in the dual cross-correlation mode. The circles represent the green cross blue correlation function, where the measured green light  $I_g(t)$  was delayed relative to the blue light  $I_b(t)$ . The squares represent the blue cross green correlation function, where  $I_b(t)$  was delayed compared with  $I_g(t)$ . It can be clearly seen from Fig. 2 that the measured  $g_c(t)$  for green cross blue is a Gaussian-like function with a baseline of 1 and that the  $g_c(t)$  for blue cross green is essentially a constant of 1 at all delay times.

Figure 2 can be understood as follows. Because the particles first pass the green and then the blue beams, delaying  $I_g(t)$  with a time interval equal to the time for the particle to cross the two laser beams will give a nonzero product of the two scattering intensities at the corresponding delay times. For other delay times the average of the product is zero, since the delay times do not match the transit time of the particles. Obviously, the blue cross green correlation function is zero in our flow configuration, because the measured  $I_b(t)$  is delayed in the wrong direction. This was further confirmed by the observation that when the flow direction is reversed, the two correlation functions shown in Fig. 2 exchange their functional forms. Figure 2 thus demonstrates that our technique is capable of distinguishing flows in two opposite directions perpendicular to the incident laser beams. This feature is useful in studies of turbulent flows, in which one can measure simultaneously the velocity probability density functions  $P(v)$  and  $P(-v)$  and study any asymme-

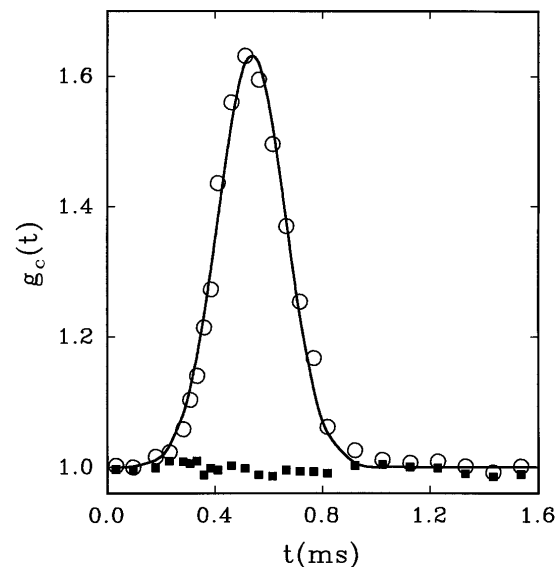


Fig. 2. Intensity cross-correlation functions  $g_c(t)$  measured in a laminar flow, with  $V_0 = 29.74 \text{ cm/s}$ : circles, green cross blue correlation function; squares, blue cross green correlation function. The solid curve is a fit to the green cross blue data. The fitted function is  $g_c(t) = 1 + 0.633 \exp\{-2[(t - 0.538 \text{ ms})/0.253 \text{ ms}]^2\}$  (see text).

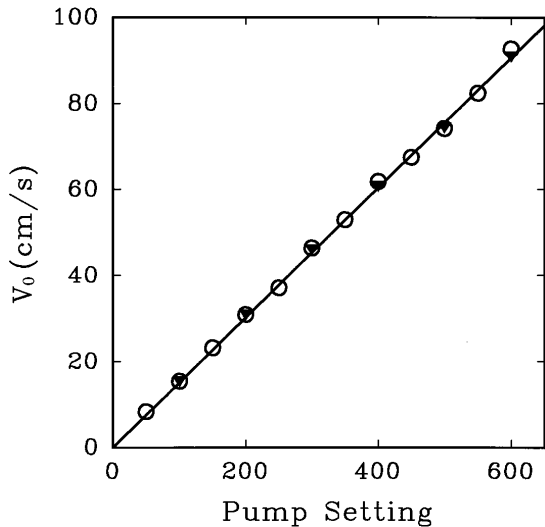


Fig. 3. Measurements of the velocity  $V_0$  at different pump settings: circles, from the measured cross-correlation function  $g_c(t)$ ; triangles, from the flow rate measurement. The solid line is a linear fit to the triangles.

try between the two density functions. The solid curve in Fig. 2 is a fitted function  $1 + A \exp[-2(t - t_0)^2/\tau^2]$ , with  $A = 0.633$ ,  $t_0 = 0.538$  ms, and  $\tau = 0.253$  ms. The functional form of the measured  $g_c(t)$  agrees well with the calculated one in Eq. (10). From the fitting above we find that  $V_0 = l/t_0 = 29.74$  cm/s, where  $l = 0.16$  mm is our beam separation.

For a laminar pipe flow the velocity at the center of the pipe  $V_0 = 2J/\pi R^2$ , where  $R = 1.8$  mm is the radius of the pipe and  $J$  is the flow rate, which can be directly measured. The triangles in Fig. 3 show the velocity  $V_0$  obtained from the measured flow rate  $J$  at different pump settings. The solid line is a linear fit to the triangles and can be used as a calibration curve for  $V_0$ . The circles in Fig. 3 represent the velocity  $V_0$  obtained from the measured  $g_c(t)$  at different pump settings. It is clearly shown in Fig. 3 that the two independent measurements are in excellent agreement with each other. This suggests that our scattering method is indeed an accurate velocimetry technique.

It is also found that the  $1/e^2$  half-width  $\tau$  of the Gaussian peak shown in Fig. 2 changes with the flow velocity  $V_0$ . Figure 4 shows the measured  $\tau$  as a function of  $V_0$ . The solid curve is the fitted function  $\tau = 7.64/V_0$  (ms), which agrees well with Eq. (10). Using the relation  $\tau = \sqrt{2}\sigma/V_0$ , we obtain the laser-beam radius  $\sigma = (7.64/\sqrt{2}) \times 10 \mu\text{m} = 54 \mu\text{m}$ , which is in excellent agreement with the direct measurement of  $\sigma$ , as discussed in Section 3. The measured  $g_{NS}(t)$  thus can be used as an accurate method to calibrate the laser-beam radius when the flow velocity is known. In the above, one obtains the beam radius  $\sigma$  by fitting the measured values of  $\tau$  as a function of  $V_0$ . In fact,  $\sigma$  can be obtained from a single measurement of  $\tau$  at a given  $V_0$  [see Eq. (10)]. The inset in Fig. 4 shows the values of  $\sigma$  obtained from the measured  $\tau$  at different velocities  $V_0$ . It clearly shows that the average value of  $\sigma$  agrees with that obtained from the fitting in Fig. 4.

As shown in Eq. (10), the amplitude of  $g_{NS}(t)$  is proportional to  $1/\bar{N}$ , where  $\bar{N}$  is the average number of

particles in the scattering volume. Figure 5 shows the measured height,  $g_c(t_0) - 1$ , of the Gaussian peak (see Fig. 2) as a function of  $\bar{N}$ . The average number  $\bar{N}$  was obtained from the known particle concentration and the calculated scattering volume from the beam radius and the slit width. The solid line in Fig. 5 represents the fitted function  $g_c(t_0) - 1 = 0.79/\bar{N}$ . Figure 5 thus confirms that the amplitude of  $g_{NS}(t)$  is indeed inversely proportional to the average number of particles in the scattering volume. To our knowledge, this is the first time that the  $\bar{N}$  dependence for number fluctuations has been measured.

To demonstrate further the capability of the technique, we measured the velocity profile across the pipe diameter for both laminar and turbulent pipe flows. In the experiment the light-collecting lens L3 (see Fig. 1) was mounted on a micrometer-controlled translation stage (Oriel model 16123). By moving the lens L3 laterally, one can conveniently project different portions of the scattering beams

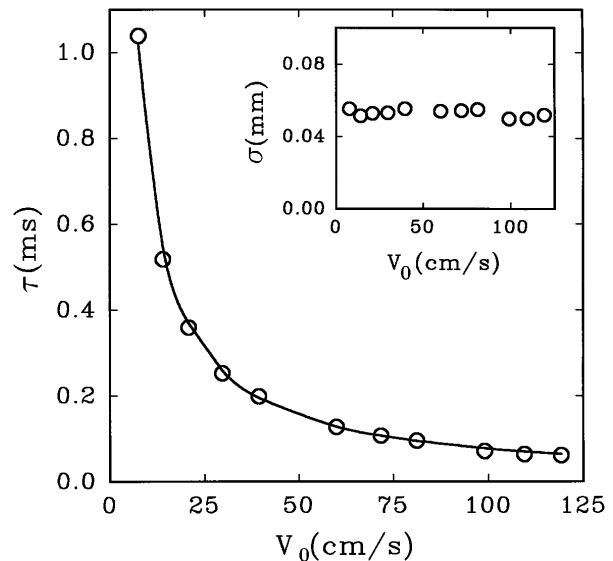


Fig. 4. Measured  $1/e^2$  half-width  $\tau$  of the Gaussian peak as a function of the velocity  $V_0$ . The solid curve is the fitted function  $\tau = 7.64/V_0$  (ms). The inset shows the laser beam radius  $\sigma$  obtained from the measured  $\tau$  at different  $V_0$ .

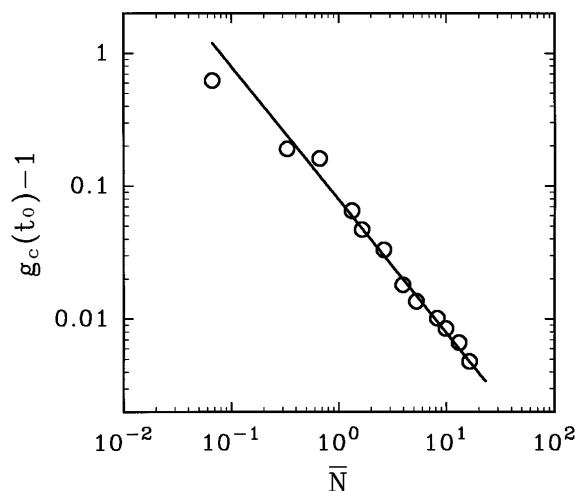


Fig. 5. Measured Gaussian peak height,  $g_c(t_0) - 1$ , as a function of the average number  $\bar{N}$  of particles in the scattering volume. Solid line, fitted function  $g_c(t_0) - 1 = 0.079/\bar{N}$ .

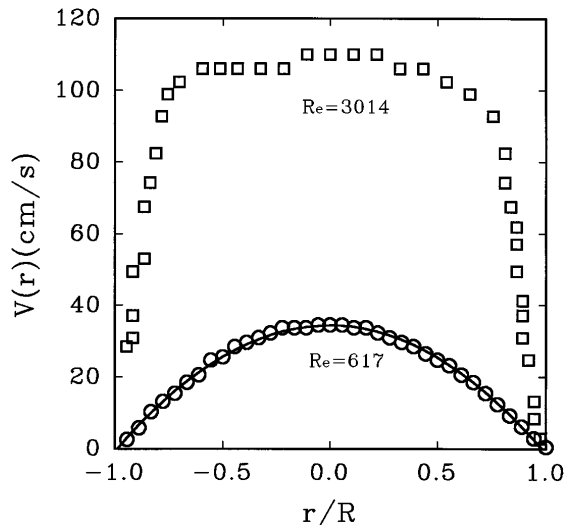


Fig. 6. Measured velocity profiles across the pipe diameter in a laminar pipe flow (circles,  $Re = 617$ ) and in a turbulent pipe flow (squares,  $Re = 3014$ ). The solid curve is a fit to the Poiseuille formula  $V(r) = V_0[1 - (r/R)^2]$  for laminar pipe flows. Here  $r$  is the radial distance from the center of the pipe,  $V_0 = 34.3$  cm/s is the velocity at  $r = 0$ , and  $R = 1.8$  mm is the inner radius of the pipe.

along the pipe diameter onto the slit. In this way the local velocity near the pipe wall can be accurately measured. Figure 6 shows the measured velocity profiles at two different flow rates. The circles were obtained at a low flow rate with the maximum velocity at the center of the pipe  $V_0 = 34.3$  cm/s. The corresponding Reynolds number  $Re = \bar{V}2R/\nu = 617$ , where  $R = 1.8$  mm is the inner radius of the pipe,  $\bar{V} = V_0/2$  is the mean velocity of the pipe flow, and  $\nu = 0.01$  cm<sup>2</sup>/s is the kinematic viscosity of water. This Reynolds number is well below the turbulent-transition Reynolds number  $Re_c$  for pipe flows ( $Re_c \approx 2000$ ).<sup>21</sup> The solid curve in Fig. 6 is a fit to the well-known Poiseuille formula  $V(r) = V_0[1 - (r/R)^2]$  for laminar pipe flows. Here  $r$  is the radial distance from the center of the pipe. The squares show the velocity profile measured at  $Re = 3014$ . This Reynolds number is larger than  $Re_c$ , and the flow is certainly in the turbulent regime. The characteristic of turbulent pipe flows is clearly shown in the measured velocity profile, which has a flat central region and a well-developed boundary layer.

The above results thus demonstrate that our technique is a convenient and accurate method for high-resolution measurements of the velocity profile and the turbulent boundary layer in the near-wall region. When the image of the scattering beam is scanned with a moving lens, it takes only  $\sim 1$  h for our technique to measure the entire velocity profile. This is much faster than the LDV technique, with which one has to move either the entire optical system or the whole flow system in order to measure the velocity profile. Unlike LDV, particle imaging velocimetry, and other time-of-flight techniques, our cross-correlation scheme is insensitive to the static background scattering from either reflecting walls or carrier fluids and therefore enhances the signal-to-noise ratio considerably unless the number of scatterers is truly overabundant.

The largest velocity that can be measured by the present technique is determined by the time resolution of the digital correlator. For our correlator (ALV-5000), a

0.1- $\mu$ s time scale can be easily resolved, which corresponds to a velocity of  $10^6$  cm/s for a 1-mm beam separation. The smallest velocity that can be measured with the technique is limited only by the Brownian diffusion of the seed particles. When the transit time for a particle to cross the two laser beams becomes longer than the time for the particle to diffuse across a beam diameter laterally, the particle will not cross the two beams in succession, and the correlation function  $g_{NS}(t) = 0$ . One can slow down the Brownian motion by using large particles. For our setup with particles 0.5  $\mu$ m in diameter, the limiting velocity is approximately  $10^{-5}$  cm/s.

When compared with the early time-of-flight techniques,<sup>6-11</sup> our new two-beam two-color scheme has the advantages of better spatial resolution and higher statistical accuracy. We extended our calculation to include the situation in which many particles are present in the scattering volumes. By signal averaging a large number of intensity fluctuations, the exact functional form of  $g_c(t)$  can be obtained with high statistical accuracy. With the ALV-5000 correlator we are able to measure fluctuating signals with a signal-to-noise ratio as low as 0.1%. From the measured  $g_c(t)$  the probability density function  $P(v)$  can be deduced. In fact, according to Eq. (11),  $P(v)$  can be obtained through a simple Laplace inversion. The only assumption used in Eq. (11) is that the laser beam has a Gaussian intensity profile. This can be directly measured with a micrometer-controlled translation stage, a small pinhole, and a photodiode. One can also calculate the cross-correlation function  $g_c(t)$  for other intensity profiles.

With the two-color scheme we are able to reduce the beam separation down to  $\sim 50$   $\mu$ m. This improvement of the spatial resolution allows us not just to measure velocity fluctuations but also to apply the technique in difficult situations in which the laser beam wanders in the fluids as a result of large fluctuations of the fluid refractive index. An example is turbulent Rayleigh-Bénard convection, in which large temperature fluctuations may cause the two defocus laser beams used in LDV to defocus and therefore reduce the signal-to-noise level. Because their smallest size ( $\sim 1$  mm) is typically much larger than the beam diameter, the temperature fluctuations will not affect the Gaussian-like nature of the beam profile but may generate small fluctuations in the beam separation. These beam-separation fluctuations introduce extra broadening in the measured correlation function  $g_c(t)$ , but the measured mean velocity will remain the same. This is because the average separation between the two laser beams is not affected by the temperature fluctuations. In the special case in which the two laser beams coincide<sup>5</sup> (a single beam consisting of two colors), the temperature fluctuations will have no effect in the measured  $g_c(t)$ .

## 5. CONCLUSION

A new dynamic light-scattering technique has been developed to measure accurately the local velocity  $v$  and its probability density function  $P(v)$ . Using two parallel laser beams of different colors, the method measures the cross-correlation function of the scattered intensities from two separate illuminating volumes. The dual-beam

two-color scheme eliminates fast phase fluctuations of the scattering intensities and is sensitive only to the intensity fluctuations caused by a seed particle that crosses the two beams in succession. The flow velocity is obtained from the measurement of the particle transit time. For a fixed beam orientation our technique is capable of distinguishing  $v$  and  $-v$ , the local velocities in the direction vertically across the two laser beams. This is because the time delay between the intensity fluctuations in the two scattering volumes, introduced by a particle crossing the two laser beams, is unidirectional. By changing the direction of the incident laser beams, one can measure the local velocity in different directions. We have devised an apparatus to rotate the two laser beams about an axis parallel and centered between them, so that the velocity component in different directions perpendicular to the laser beams can be easily measured. We have framed the scattering theory so as to account for the fluctuations in the number of particles in the two-beam scattering geometry. Our experiment verifies the calculation and demonstrates applications of the technique. The advantages of the technique are its high spatial resolution and accuracy, fast temporal response, and ease of use. In studies of turbulent flows the method can be used to measure the probability density functions  $P(v)$  and  $P(-v)$  simultaneously. We also expect this method to be useful in studies of near-wall turbulence, sedimentation of heavy particles, and flow phenomena in complex fluids, for which detection of minute velocity changes is of interest.

## ACKNOWLEDGMENTS

We thank B. J. Ackerson for useful discussions. K.-Q. Xia gratefully acknowledges partial support of this work by the Research Grants Council of Hong Kong through a Direct Grant for Research 1993/1994 (220600470). P. Tong acknowledges support from the National Science Foundation under grant DMR-9312398. He also acknowledges the kind hospitality of, and the C. N. Yang Visiting Fellowship from, the Physics Department of the Chinese University of Hong Kong during his stay.

## REFERENCES

1. E. D. Siggia, "High Rayleigh number convection," *Ann. Rev. Fluid Mech.* **26**, 137–168 (1994).
2. J.-Z. Xue, E. Herbolzheimer, M. A. Rutgers, W. B. Russel, and P. M. Chaikin, "Diffusion, dispersion, and settling of hard spheres," *Phys. Rev. Lett.* **69**, 1715–1718 (1992).
3. T. C. Van Vechten and C. Franck, "Relative importance of convection and diffusion in binary liquid systems subject to small horizontal temperature gradients," *Phys. Rev. E* **48**, 3635–3642 (1993).
4. F. Durst, A. Melling, and J. H. Whitelaw, *Principles and Practice of Laser-Doppler Anemometry*, 2nd ed. (Academic, New York, 1981).
5. P. Tong, K.-Q. Xia, and B. J. Ackerson, "Incoherent cross-correlation spectroscopy," *J. Chem. Phys.* **98**, 9256–9265 (1993).
6. R. Schodl, "Laser-two-focus (L2F) for use in aero engines," *AGARD Lect. Ser.* **90**, 4.1–4.34 (1977).
7. L. Lading, A. Skov Jensen, C. Fog, and H. Andersen, "Time-of-flight laser anemometer for velocity measurements in the atmosphere," *Appl. Opt.* **17**, 1486–1488 (1978).
8. R. Schodl, "Laser-two-focus velocimetry," *AGARD Conf. Proc.* **399**, 7.1–7.31 (1986).
9. L. Lading, "The time-of-flight laser anemometer," *AGARD Conf. Proc.* **193**, 23.1–23.20 (1976).
10. K. G. Bartlett and C. Y. She, "Single-particle correlated time-of-flight velocimeter for remote wind-speed measurement," *Opt. Lett.* **1**, 175–177 (1977).
11. C. Y. She and R. F. Kelley, "Photon-burst correlation techniques for atmosphere crosswind measurements," *Appl. Phys. B* **33**, 195–204 (1984).
12. B. J. Berne and R. Pecora, *Dynamic Light Scattering* (Wiley, New York, 1976).
13. P. N. Pusey, "Statistical properties of scattered radiation," in *Photon Correlation Spectroscopy and Velocimetry*, H. Z. Cummins and E. R. Pike, eds. (Plenum, New York, 1977).
14. P. N. Pusey, "Number fluctuations of interacting particles," *J. Phys. A* **12**, 1805–1818 (1979).
15. See, e.g., *Photon Correlation Spectroscopy and Velocimetry*, H. Z. Cummins and E. R. Pike, eds. (Plenum, New York, 1977).
16. G. G. Fuller, J. M. Rallison, R. L. Schmidt, and L. G. Leal, "The measurement of velocity gradients in laminar flow by homodyne light-scattering spectroscopy," *J. Fluid. Mech.* **100**, 555–575 (1980).
17. P. Tong and W. I. Goldburg, "Experimental study of relative velocity fluctuations in turbulence," *Phys. Lett. A* **127**, 147–150 (1988); W. I. Goldburg, P. Tong, and H. K. Pak, "A light scattering study of turbulence," *Physica D* **38**, 134–140 (1989).
18. N. A. Clark, B. J. Ackerson, and A. J. Hurd, "Multidetector scattering as a probe of local structure in disordered phases," *Phys. Rev. Lett.* **50**, 1459–1462 (1983).
19. B. J. Ackerson, T. W. Taylor, and N. A. Clark, "Characterization of the local structure of fluids by apertured cross-correlation functions," *Phys. Rev. A* **31**, 3183–3193 (1985).
20. D. W. Schaefer and B. J. Berne, "Number fluctuation spectroscopy of motile microorganisms," *Biophys. J.* **15**, 785–794 (1975).
21. D. J. Tritton, *Physical Fluid Dynamics*, 2nd ed. (Oxford, London, 1988).